

# Climate change scenarios of heat waves in Central Europe and their uncertainties

Ondřej Lhotka<sup>1,2,3</sup>  · Jan Kyselý<sup>1,4</sup> · Aleš Farda<sup>2,5</sup>

Received: 31 May 2016 / Accepted: 27 December 2016 / Published online: 7 January 2017  
© Springer-Verlag Wien 2017

**Abstract** The study examines climate change scenarios of Central European heat waves with a focus on related uncertainties in a large ensemble of regional climate model (RCM) simulations from the EURO-CORDEX and ENSEMBLES projects. Historical runs (1970–1999) driven by global climate models (GCMs) are evaluated against the E-OBS gridded data set in the first step. Although the RCMs are found to reproduce the frequency of heat waves quite well, those RCMs with the coarser grid (25 and 50 km) considerably overestimate the frequency of severe heat waves. This deficiency is improved in higher-resolution (12.5 km) EURO-CORDEX RCMs. In the near future (2020–2049), heat waves are projected to be nearly twice as frequent in comparison to the modelled historical period, and the increase is even larger for severe heat waves. Uncertainty originates mainly from the selection of RCMs and GCMs because the increase is similar for all concentration scenarios. For the late twenty-first century (2070–2099), a substantial increase in heat wave frequencies is projected, the magnitude of which depends mainly upon concentration scenario. Three to four heat waves per summer are

projected in this period (compared to less than one in the recent climate), and severe heat waves are likely to become a regular phenomenon. This increment is primarily driven by a positive shift of temperature distribution, but changes in its scale and enhanced temporal autocorrelation of temperature also contribute to the projected increase in heat wave frequencies.

## 1 Introduction

Heat waves are one of the main concerns in relation to the ongoing climate change. The severity of heat waves has increased across European regions in the recent decades (Della-Marta et al. 2007; Kyselý 2010; Valeriánová et al. 2015). The most notable events occurred in 2003 over Western Europe (Fink et al. 2004) and in 2010 over Eastern Europe and Russia (Schneidereit et al. 2012). Recently, Central Europe was affected by several extraordinary heat waves in the summer of 2015, during which the highest historically recorded daily maximum temperature ( $T_{\max}$ , 40.3 °C) was measured in Germany (DWD 2015), and majority of heat wave indices in this summer exhibited record-breaking values over the region (Hoy et al. 2016). Central Europe experienced severe heat waves also in summer 2013, which ranked as the eighth most extreme since 1951 at the continental scale, and the heat wave severity broke historical records at several stations with long-term measurement (Lhotka and Kyselý 2015b). In 2013, the highest historically recorded  $T_{\max}$  (40.5 °C) was reached in Austria (ZAMG 2013), and the highest temperature for the Czech Republic (40.4 °C) was observed 1 year earlier, in August 2012, during a relatively short heat wave (Holtanová et al. 2015). It is estimated that the probability of severe heat waves such as the 2003 heat wave over Western Europe has increased by a factor of 2–4 due to climate change (Coumou

**Electronic supplementary material** The online version of this article (doi:10.1007/s00704-016-2031-3) contains supplementary material, which is available to authorized users.

✉ Ondřej Lhotka  
ondrej.lhotka@ufa.cas.cz

- <sup>1</sup> Institute of Atmospheric Physics CAS, Prague, Czech Republic
- <sup>2</sup> Global Change Research Institute CAS, Brno, Czech Republic
- <sup>3</sup> Faculty of Science, Charles University, Prague, Czech Republic
- <sup>4</sup> Faculty of Environmental Sciences, Czech University of Life Sciences, Prague, Czech Republic
- <sup>5</sup> Czech Hydrometeorological Institute, Prague, Czech Republic

and Rahmstorf 2012), and Fischer and Knutti (2015) concluded that about 75% of hot extremes over land areas worldwide in the past six decades are attributable to the observed warming.

Heat waves cause excess illness and mortality, losses in agricultural production, forest fires, increased energy demand for cooling and other related hazards (Beniston et al. 2007), and there is growing evidence that the European agricultural sector will need to adopt suitable adaptation strategies in relation to more frequent heat stress (Iglesias et al. 2012). The 2003 heat waves caused 70,000 excess deaths in Europe, mainly in the elderly population (Robine et al. 2008), and the 2010 heat wave in Russia was associated with a death toll of 55,000 (Barriopedro et al. 2011). Bastos et al. (2014) showed that both events led to a marked decrease of plant productivity. In addition, numerous wildfires that occurred in 2010 caused continuous episodes of extreme air pollution in several Russian cities (Konovalov et al. 2011).

In general, heat waves are expected to become more frequent, more intense and longer lasting in a future climate (Meehl and Tebaldi 2004; Lau and Nath 2014; Lemonsu et al. 2014). More specifically, based on ENSEMBLES regional climate models (RCMs) driven by global climate models (GCMs) forced by the SRES A1B scenario, Fischer and Schär (2010) showed that the occurrence of heat waves is projected to increase substantially by the end of the twenty-first century in most European regions and their peak temperature may be enhanced by approximately 5 °C. These changes are usually reported to be driven rather by higher mean temperature than by larger temperature variability (Ballester et al. 2010). There is nevertheless a considerable spread among individual climate models, causing substantial uncertainties in future projections.

The evaluation of uncertainties is fundamental for any application (Déqué et al. 2012) and presents a key challenge for adaptation planning. Uncertainties in climate projections originate from three main sources: the choice of emission/concentration scenario, internal variability of climate and model uncertainties (Hawkins and Sutton 2009). Concentration scenarios represent possible ways of human society's development that alter a radiative forcing on climate (Moss et al. 2010), mainly through a modification of atmospheric chemistry and land-cover changes. In the extratropics, the uncertainty based on internal climate variability is mainly associated with atmospheric dynamics, dominated by teleconnection modes (Deser et al. 2012), such as the North Atlantic Oscillation (Hurrell and Deser 2010). The model uncertainty arises from the nature of model design, as different RCMs exhibit various internal behaviours and their simulations are driven by different GCMs.

Identifying typical features of individual models related to heat waves in the historical climate are crucial for credible interpretation of their projections. Kjellström et al. (2007)

demonstrated that RCMs tend to underestimate high summer temperatures over Scandinavia and the British Isles, while an overestimation was found over Eastern Europe, the Mediterranean and the Iberian Peninsula. Kjellström et al. (2011) attributed the negative temperature bias in the northern parts of the European domain to improper simulation of sea surface temperature and ice condition in the North Atlantic, while the positive temperature bias in the south was triggered by too-dry model climate in the spring and summer in the Mediterranean. In Central Europe, a negative bias of daily maximum temperature is often reported (Nikulin et al. 2011; Plavcová and Kyselý 2011), but Kjellström et al. (2010) showed that this bias is one of the smallest across the European domain. Reproduction of heat waves nevertheless requires not only a good simulation of the right tail of a temperature distribution but also the persistence of high temperatures. The capability of RCMs to simulate heat waves over Europe was evaluated by Vautard et al. (2013), who found that biases in modelled temperature influenced characteristics of heat waves that were too persistent and severe. A different approach to defining heat waves was adopted by Lhotka and Kyselý (2015c), who took into account their temperature magnitude, length and spatial extent. Simulated heat waves were then shorter but more frequent, and their peak temperatures were substantially overestimated.

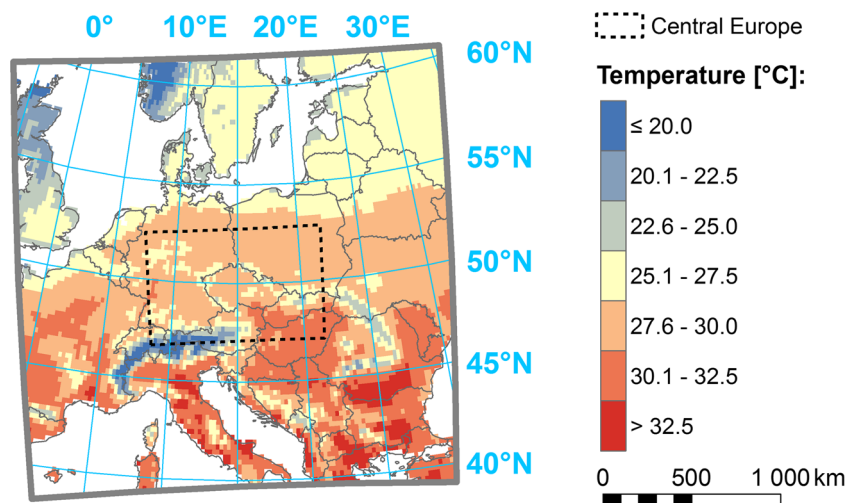
Previous studies on climate change scenarios have not evaluated in detail the aforementioned uncertainties when analysing heat waves in a future climate. The focus of the present study is on uncertainties connected with the choice of emission/concentration scenario (RCP 4.5, RCP 8.5 and SRES A1B), model resolution (12.5, 25 and 50 km) and the climate model (31 RCM × GCM combinations). The changes and uncertainties are assessed for the near future (2020–2049) and the late twenty-first century (2070–2099). An evaluation of the RCMs is performed against the E-OBS gridded data set over the 1970–1999 historical period. Since the study involves a large ensemble of RCMs with various characteristics, this approach allows analysing magnitude of projected changes with respect to the related uncertainties.

## 2 Data and methods

### 2.1 Area of interest and observed data

Heat waves are analysed over Central Europe that is situated approximately between 47 and 53° N and 8 and 22° E (Fig. 1). The area contains 4160 (80 × 52), 1040 (40 × 26) or 260 (20 × 13) grid points, depending on horizontal grid spacing of a particular data (12.5, 25 or 50 km, respectively). This region's location is designed for the most common rotated pole grid and is identical for observed data and all three horizontal grid spacings of the RCMs. It is analogous to that used

**Fig. 1** Definition of Central Europe (black dashed polygon) and the 90th percentile of summer daily maximum temperature calculated for the 1970–1999 period (colour shading) in the E-OBS 11.0 gridded data set



in the previous study focused on evaluation of heat waves in RCM simulations (Lhotka and Kysely 2015c). The E-OBS 11.0 gridded data set (0.22 rotated grid, Haylock et al. 2008) is used as a source of observations. This data set covers whole continental Europe over the 1950–2014 period, but the evaluation of model simulations is performed during the shorter 1970–1999 period due to the limited time span of modelled data.

## 2.2 Climate model simulations

Modelled data are taken from the EURO-CORDEX (Jacob et al. 2014) and ENSEMBLES (van der Linden and Mitchell 2009) projects. While EURO-CORDEX provides RCM simulations in 50 and 12.5 km resolutions driven by Representative Concentration Pathways (RCP) scenarios (van Vuuren et al. 2011), the ENSEMBLES project is valuable in that it provides RCMs in the 25 km resolution forced by the SRES A1B scenario (Arnell et al. 2004). Individual RCMs had been subjected to various upgrades during the time period between the ENSEMBLES project phase and the EURO-CORDEX simulations. The EURO-CORDEX models investigated in this study had improved their respective sets of physical parameterizations while keeping their basic principles from the ENSEMBLES stage. Another change is the use of more recent surface property data sets and improved restart techniques, for example, in RCA4 (Strandberg et al. 2014) and CLM RCMs (Davin et al. 2011). The majority of the model simulations are available up to the end of the twenty-first century (Table 1), and all simulations have available their historical runs (1970–1999) driven by the same GCM.

Individual model simulations from the EURO-CORDEX project are listed in Online Resource 1. These models have 0.11° (12.5 km) or 0.44° (50 km) horizontal grid spacing and are forced by the RCP 4.5 or RCP 8.5 scenarios. The RCP 4.5 scenario represents stabilization of concentrations without

overshooting effective radiative forcing (ERF) of 4.5 W/m<sup>2</sup> relative to pre-industrial values (~650 ppm CO<sub>2</sub> equivalent). This is achieved by implementing mitigation policies (Thomson et al. 2011). The total ERF is 2.3 W/m<sup>2</sup> in year 2020, 3.4 W/m<sup>2</sup> in 2050, 3.8 W/m<sup>2</sup> in 2070 and 3.9 W/m<sup>2</sup> in 2100 (Prather et al. 2013). By contrast, the RCP 8.5 scenario represents a long-term large energy demand without implementation of mitigation policies, thus leading to high greenhouse gas emissions (Riahi et al. 2011). This scenario is presumed to reach an ERF of 8.5 W/m<sup>2</sup> (~1370 ppm CO<sub>2</sub> equivalent) and the total anthropogenic ERF is 2.3 W/m<sup>2</sup> in the year 2020, 4.4 W/m<sup>2</sup> in 2050, 5.9 W/m<sup>2</sup> in 2070 and 8.0 W/m<sup>2</sup> in 2100 (Prather et al. 2013). It should be mentioned that the EURO-CORDEX ensemble may be unbalanced due to the majority of RCA4 RCM simulations (especially in the 0.44° grid), which has to be taken into account when interpreting the model outputs.

Sixteen RCM simulations that use rotated grid and the 0.22° (25 km) horizontal grid spacing were taken from the ENSEMBLES project (Online Resource 2). These simulations are forced by the SRES A1B concentration scenario that represents rapid economic growth with increasing globalization, fast

**Table 1** Number of model simulations from the EURO-CORDEX and ENSEMBLES projects for the near future and the late twenty-first century

	2020–2049	2070–2099
CORDEX—0.11°—RCP 4.5 W m <sup>-2</sup>	10	10
CORDEX—0.11°—RCP 8.5 W m <sup>-2</sup>	10	10
CORDEX—0.44°—RCP 4.5 W m <sup>-2</sup>	13	13
CORDEX—0.44°—RCP 8.5 W m <sup>-2</sup>	13	13
ENSEMBLES—0.22°—SRES A1B	16	13
Total	62	59

Decimal numbers represent the horizontal grid spacing; ‘RCP’ or ‘SRES’ denote the concentration scenario

technological change and low population increase (Arnell et al. 2004). The total anthropogenic ERF is  $2.2 \text{ W/m}^2$  in the year 2020,  $4.2 \text{ W/m}^2$  in 2050,  $5.3 \text{ W/m}^2$  in 2070 and  $6.0 \text{ W/m}^2$  in 2100 (Prather et al. 2013).

In some studies, a relatively large numbers of gaps in RCM  $\times$  GCM matrices were completed using statistical methods for data reconstruction. Nevertheless, Heinrich et al. (2014) showed that seasonal mean climate change of the ENSEMBLES RCM projections is not significantly biased due to the lack of driving GCMs. This technique is therefore not employed in the present study, and we analyse only the available simulations.

### 2.3 Definition of heat wave

Heat waves are defined with respect to their temperature magnitude, length and spatial extent. First, all data are recalculated to the  $0.44^\circ$  (50 km) grid through averaging four (16) respective grid cells when transforming the original 25 km (12.5 km) grid. Inasmuch as a sensitivity study had shown the occurrence of heat waves to be identical in selected  $0.22^\circ$  (25 km) data sets and in their recalculated  $0.44^\circ$  versions, we found this approach useful for direct comparison of heat wave characteristics among all data sets involved. An analogous procedure was applied by Kotlarski et al. (2014) when comparing the performance of EURO-CORDEX and ENSEMBLES models driven by reanalyses. We note that some heat wave characteristics (e.g. temperature amplitude) cannot be directly compared between different resolutions, and this approach also overcomes the issue with the missing observed  $0.11^\circ$  (12.5 km) grid data for the evaluation of historical runs.

The definition of heat waves is based on the occurrence of hot days over Central Europe and is similar to that proposed by Lhotka and Kyselý (2015a). A heat wave is defined by at least three consecutive hot days. A hot day occurs when the average of  $T_{\max}$  deviations from the 90th percentile of their summer distribution is positive over Central Europe (calculated in the 1970–1999 period). The percentiles are calculated individually for observed data and each model simulation in order to remove the influence of a  $T_{\max}$  bias. This approach is suitable when focusing rather on the behaviour of the right tail of the  $T_{\max}$  distribution and the spatial and temporal structure of daily temperatures (which are essential for heat waves) than on the  $T_{\max}$  bias itself. The use of the respective percentiles has already been employed in previous studies (Ballester et al. 2010; Fischer and Schär 2010; Vautard et al. 2013). We note that although simulated values of  $T_{\max}$  are affected by elevation differences among their original grids ( $0.11^\circ$ ,  $0.22^\circ$  and  $0.44^\circ$ ), it is not necessary to perform a  $T_{\max}$  elevation correction since the percentiles are calculated separately for each RCM simulation.

In future time slices, the calculated percentiles from the historical period are kept. Although future society may regard

heat waves that are considered severe in the present climate as ordinary under climate change conditions due to its adaptation, we found this approach useful to illustrate possible changes of heat waves relative to historical climate. Moreover, heat waves pose a threat also for ecosystems, which ability to adapt may be limited.

### 2.4 Heat wave characteristics

Four characteristics of a heat wave are calculated so that each event is described by (i) temperature amplitude, (ii) length, (iii) spatial extent and (iv) extremity index. Temperature amplitude is the highest daily  $T_{\max}$  excess above the 90th percentile of the summer  $T_{\max}$  distribution during a heat wave (at any grid point in Central Europe) and represents the temperature anomaly of its peak. Length is the number of consecutive hot days that form a heat wave (minimum of three hot days). Spatial extent is represented by an area where  $T_{\max}$  deviations above the 90th percentile of summer  $T_{\max}$  distribution are positive for at least three successive days, and it is given as a ratio (1.0 means that whole Central Europe is affected by a heat wave). The extremity index is adopted from Lhotka and Kyselý (2015a) and is defined as a sum of positive  $T_{\max}$  deviations in all Central European grid points during a heat wave, scaled by the total number of (recalculated) grid points over Central Europe (260). This index captures joint effects of temperature, length and spatial extent of heat waves. An example of the heat wave definition and calculation of its characteristics is given in Fig. 2.

### 2.5 Temporal autocorrelation and statistical testing

Analogously to Lhotka and Kyselý (2015c), persistence of  $T_{\max}$  over Central Europe, which is an important aspect for heat wave development, is analysed by temporal autocorrelation computed as the Pearson product moment coefficients for lagged data pairs. For each day in the summer,  $T_{\max}$  values across 260 grid points over Central Europe are averaged into a

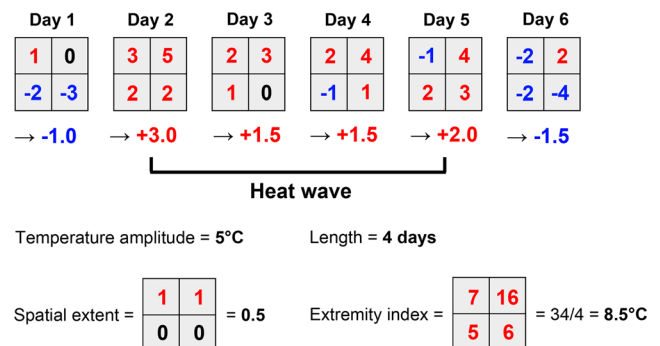


**Fig. 2** Theoretical example of the heat wave definition and calculation of heat wave characteristics over a hypothetical area represented by four grid points. Positive (red), negative (blue) and zero (black) deviations from the 90th percentile of summer  $T_{\max}$  distribution are shown

regionally averaged  $T_{\max}$ , which is used to compute correlation coefficients. Since the summer  $T_{\max}$  series is not continuous, we calculated correlation coefficients ( $r$ ) individually for each summer. Because a simple arithmetic mean of (seasonal) correlation coefficients may be underestimated due to a skewed distribution (Silver and Dunlap 1987), Fisher's  $z$  transformation was applied before averaging with the following equation:

$$z = 0.5 \log_e \left( \frac{1+r}{1-r} \right).$$

The mean of  $z$  values was then back transformed using an inverse function to the Fisher's transformation. Statistical significance of changes in temporal autocorrelation was assessed using the two-sided Wilcoxon rank sum test. This non-parametric test is chosen because the criterion of data normality is not always met.

### 3 Observed heat waves and evaluation of historical RCM simulations

Because the study includes evaluating performance of the RCMs' historical simulations, observed heat wave characteristics are analysed first. In the E-OBS data, 22 heat waves are found in the 1970–1999 period (7.3 heat waves per decade). Their temperature amplitude ranges from 4.1 to 9.8 °C, the length varies from 3 days (by definition) to 16 days, the spatial extent ranges from 0.24 to 1 and the extremity index varies from 2.5 to 51.4 °C. Median values of heat wave characteristics are 5.7 °C (temperature amplitude), 4 days (length), 0.64

(spatial extent) and 7.4 °C (extremity index, Fig. 3). Hereafter, a heat wave is considered 'severe' when all its characteristics are equal to or exceed these median values.

Only 5 of the 22 heat waves (in 1971, 1974, 1976, 1992 and 1994) meet this severe heat wave criterion (1.7 severe heat waves per decade). The heat wave of 1994 is exceptional due to its length (16 days) and a very high extremity index. This long-lasting event affected whole Central Europe, but its temperature amplitude is not extremely pronounced (Fig. 3). Larger-scale temperature patterns associated with each severe heat wave are shown in Fig. 4.

Evaluation of simulated frequencies of heat waves and severe heat waves is performed individually for (i) EURO-CORDEX RCMs with the 0.11° grid, (ii) EURO-CORDEX RCMs with the 0.44° grid and (iii) ENSEMBLES RCMs with the 0.22° grid. These groups are hereafter referred to as COR11, COR44 and ENS22, respectively. In all three groups, frequencies of 'all' heat waves are reproduced considerably better compared to severe heat waves. Although a large variance is present in ENS22, the observed frequency of heat waves (7.3/decade) fits into the simulated interquartile range (IQR). The IQR in COR11 and COR44 is beyond the observed frequency, but the variance is smaller and no substantial outliers are present in COR11. For severe heat waves, a large overestimation of their frequencies is found, which is mainly linked to substantial overestimation of median temperature amplitude in the RCMs. Although the observed frequency of severe heat waves (1.7/decade) is located in the lower quartile in all three RCM groups (Fig. 5a–c), the higher-resolution COR11 performed best, because the RCMs in this group are able to capture median spatial extent of heat waves reasonably well. On the other hand, an event with equal or higher characteristics compared to the

**Fig. 3** Histograms of heat wave characteristics (temperature amplitude, length, spatial extent, extremity index) for observed heat waves in the 1970–1999 period. Green vertical lines represent median values and red vertical lines indicate values for the extraordinary 1994 heat wave

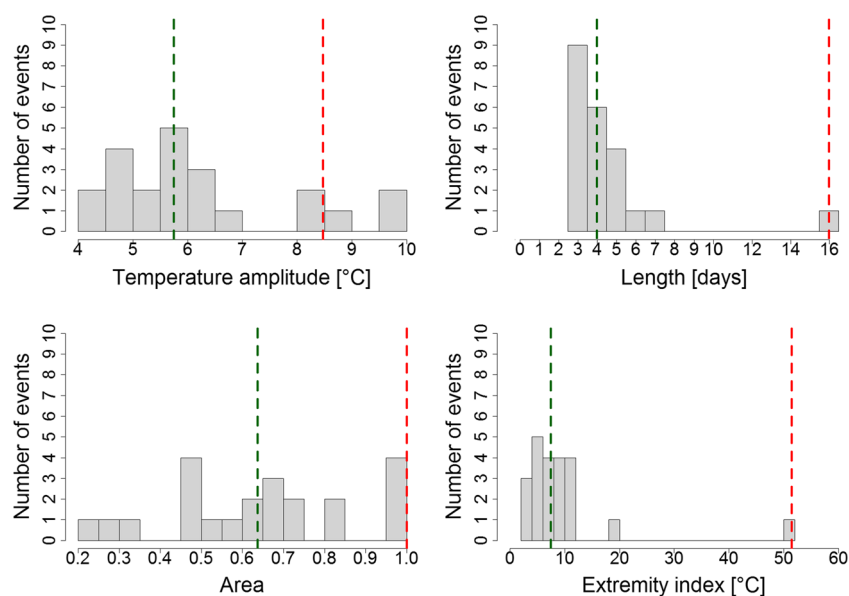
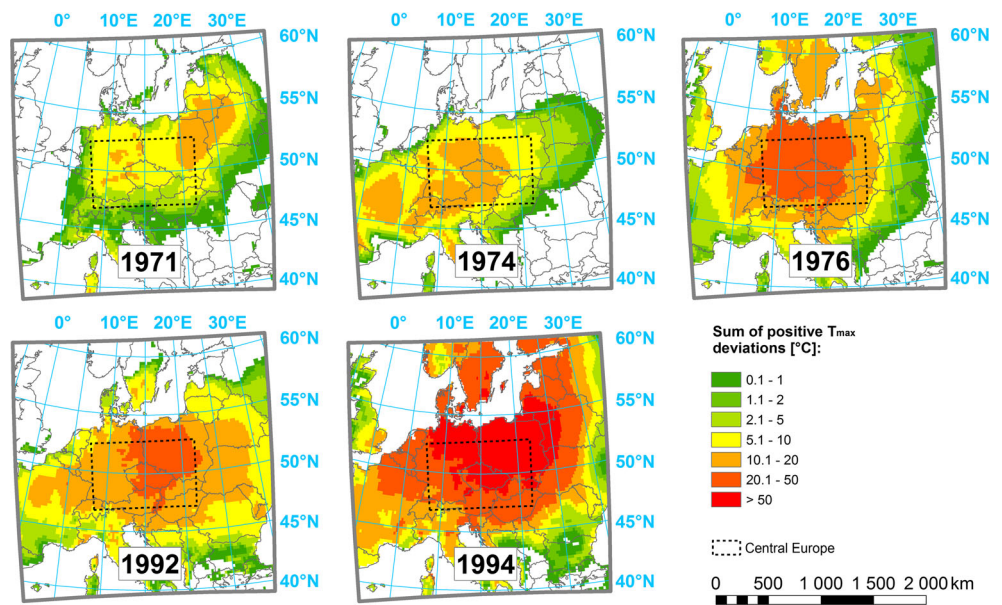


**Fig. 4** Severe heat waves over Central Europe during the 1970–1999 period. *Colour shading* represents the sum of positive  $T_{max}$  deviations from the 90th percentile of its summer distribution. Note that only grid points located within the Central European domain are used to compute heat wave characteristics



exceptional heat wave that occurred in 1994 (temperature amplitude = 8.5 °C, length = 16 days, spatial extent = 1.0,

extremity index = 51.4 °C) was found only in 3 of the 39 model simulations for the historical period.

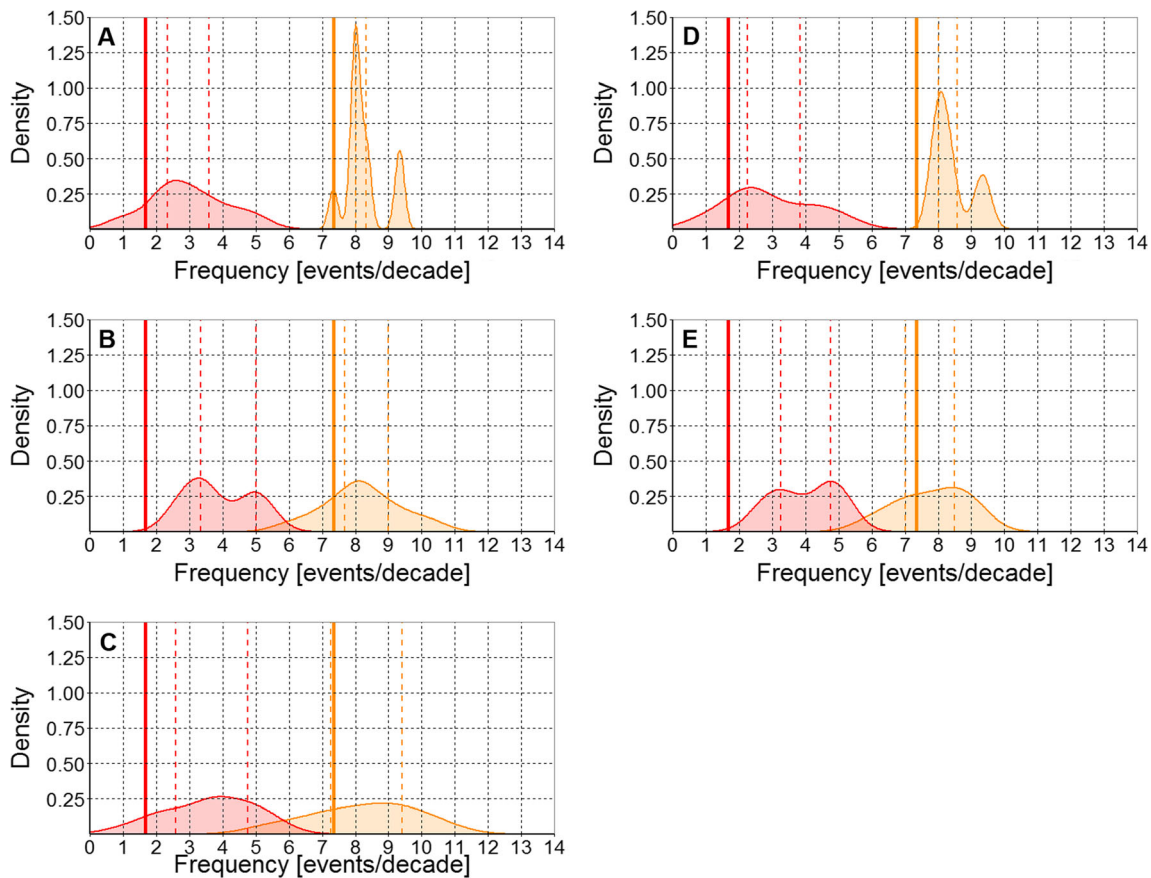


**Fig. 5** Probability density functions (PDFs) of heat waves (*orange*) and severe heat waves (*red*) frequencies for **a** COR11, **b** COR44 and **c** ENS22. EURO-CORDEX models that are available in both grids (which allows for a fair comparison) are shown in **d** the 0.11° grid and

**e** the 0.44° grid. *Solid vertical lines* represent the frequency in E-OBS while *dashed vertical lines* delimit the interquartile ranges of model historical simulations

Changes in temporal autocorrelation of regionally averaged  $T_{\max}$  (hereafter simply referred as autocorrelation) are assessed for lags from 1 to 10 days. In E-OBS, the autocorrelation for lag 1 is 0.86 and then it decreases exponentially to 0.06 for lag 10. COR11 and COR44 (historical simulations) significantly underestimate the autocorrelation for the first two lags (Table 2). This underestimation is particularly pronounced and highly significant for the lag of 1 day (at the 1% significance level). By contrast, the autocorrelation was overestimated from lag 5 compared to E-OBS, but these changes are found to be insignificant. In ENS22, the autocorrelation is significantly enhanced for lags 4–9, while the underestimation for lag 1 is small and insignificant (Table 2).

In order to investigate an effect of model resolution on the simulation of heat wave and severe heat wave frequencies, eight models from the EURO-CORDEX project which are available in both grids (Online Resource 1) were selected (Fig. 5d, e). The overall patterns of probability density functions (PDFs) are similar to those in Fig. 5a, b, which means that the differences between COR11 and COR44 are related to different model resolutions rather than different composition of ensembles in these groups.

#### 4 Heat wave scenarios and uncertainties for near future and late twenty-first century

In the near future time slice (2020–2049), both heat waves and severe heat waves are projected to become more frequent in comparison to the modelled historical climate (1970–1999). Relatively large uncertainty was found, inasmuch as the IQRs for frequencies of these events are considerably widened compared to the historical simulations. The largest increment of the heat wave frequency is present in EURO-CORDEX groups forced by the ‘low concentration’ RCP 4.5 scenario; however, it should be noted that differences among scenarios are small in this period. There is no clear dependence on model resolution because in both COR11 and COR44 groups,

heat waves and severe heat waves are projected to be more enhanced under RCP 4.5 (Fig. 6).

The frequency of heat waves is projected to be nearly twice higher compared to the modelled historical period. The largest increase is found for COR44 forced by RCP 4.5, which relates to the largest change in the scale parameter (i.e. the largest increment in variance) of the  $T_{\max}$  distribution and also enhanced temporal autocorrelation (Table 3). Although the increase in median  $T_{\max}$  is comparable across all model groups, the location of the 90th percentile is particularly shifted in COR44 forced by RCP 4.5. The lowest increment of the heat wave frequency was present in ENSEMBLES simulations, which corresponds with generally negative changes in temporal autocorrelation of  $T_{\max}$  and only a small positive change of the scale. A link between the increment of heat waves and changes in temporal autocorrelation is poorly expressed in this period, compared to the shift of the 90th percentile (Online Resource 3).

In general, severe heat waves are expected to be more enhanced than heat waves (by a factor of 2–3 compared to historical simulations) and their frequency is projected to become comparable to the frequency of all heat waves in the 1970–1999 period. It should be emphasized, however, that the model simulations considerably overestimated the severe heat wave frequencies in the recent climate, and thus, this projection might be biased. Analogously to the historical period, the frequency of exceptional events with magnitude equal to or higher than the 1994 heat wave is analysed. In the 30-year period 2020–2049, 29 of the 62 model simulations project at least one such event and six RCM simulations project this type of event to occur at least once per decade. These exceptional heat waves are found in all model groups, and they are not linked to specific concentration scenarios. Despite the substantial increment of these events compared to the historical simulations, they are still rather rare in the near future projections.

Changes of heat wave and severe heat wave frequencies are clearly linked to the concentration scenarios in the late twenty-first century time slice (2070–2099). The largest increases of these events are found in COR11 and COR44 driven by RCP 8.5. In these groups, the frequency of heat waves is projected to be enhanced by a factor of 4–5 compared to the historical simulations, indicating 3–4 heat waves per year on average at the end of the twenty-first century. By contrast, the increase in the heat wave occurrence is roughly halved under the RCP 4.5 scenario (about two heat waves per year on average). ENS22, with the SRES A1B scenario, projects an increase between the two RCP scenarios, which is in line with the average effective radiative forcing for 2070–2099 (Fig. 7). The largest increment under RCP 8.5 is related to a large shift of the  $T_{\max}$  distribution and positive significant changes in temporal autocorrelation of  $T_{\max}$  (Table 4). A relationship between the increment of heat waves and changes in temporal

**Table 2** Temporal autocorrelation of summer daily maximum temperature for the historical period (1970–1999)

	L1	L2	L3	L4	L5	L6	L7	L8	L9	L10
E-OBS	0.86	0.62	0.42	0.31	0.22	0.18	0.15	0.11	0.09	0.06
COR11	<b>0.80</b>	0.55	0.40	0.31	0.25	0.20	0.16	0.13	0.11	0.10
COR44	<b>0.80</b>	0.55	0.39	0.30	0.24	0.19	0.16	0.13	0.11	0.09
ENS22	0.85	0.63	0.47	0.38	0.33	0.27	0.22	0.19	0.16	0.11

COR11 (COR44) represents EURO-CORDEX models with 0.11° (0.44°) grids and ENS22 denotes ENSEMBLES models with 0.22° grid. L1–L10 represents lags from 1 to 10 days, italicised (bolded) values are significantly different from E-OBS at the 5% (1%) significance level

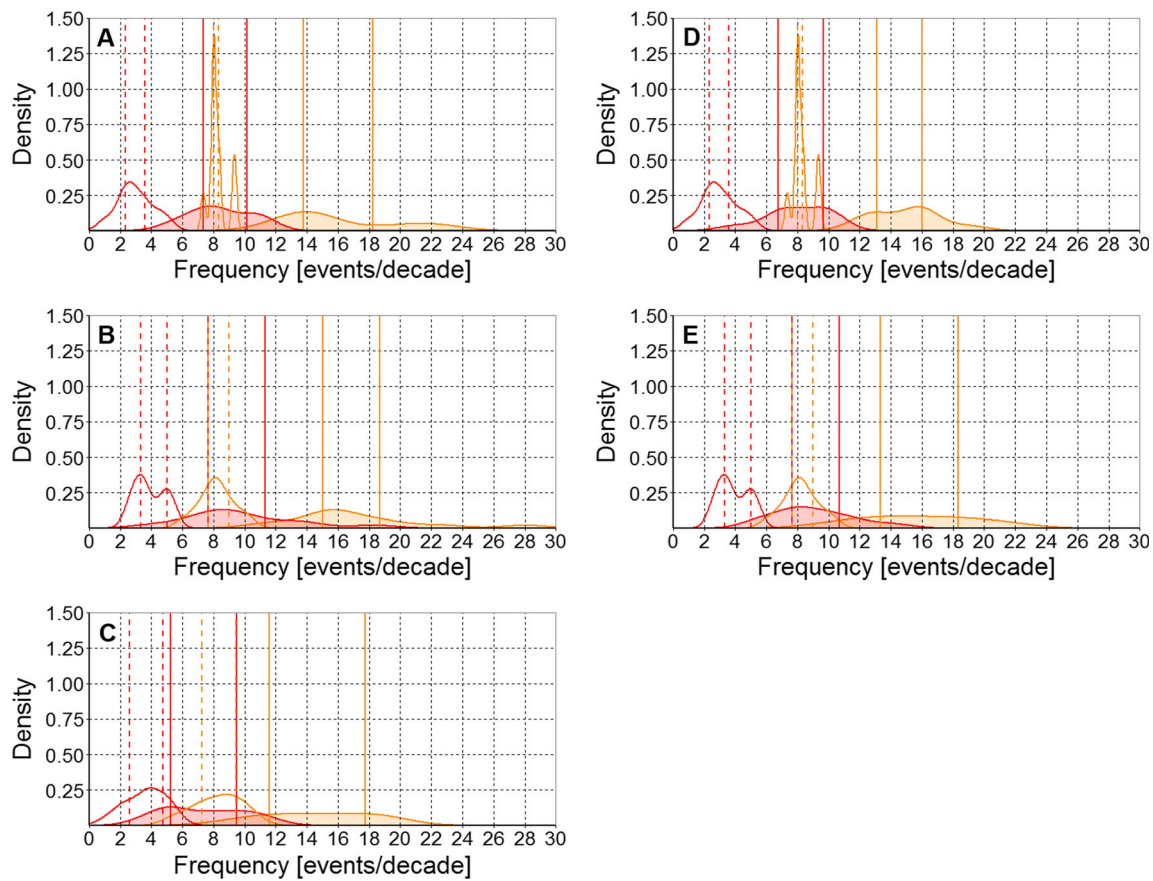


**Fig. 6** Probability density functions (PDFs) of heat waves (*orange*) and severe heat waves (*red*) frequencies for **a, b** COR11 and COR44 forced by the RCP 4.5 scenario, **c** ENS22 forced by the SRES A1B scenario and **d, e** COR11 and COR44 forced by the RCP 8.5 scenario (*shaded curves*).

*Unshaded curves* represent historical simulations. *Solid vertical lines* delimit the interquartile ranges of model simulations for the near future while *dashed vertical lines* represent the interquartile ranges of model simulations for the historical runs

autocorrelation is tighter in this period compared to near future, but still relatively weak (Online Resource 4).

A similar pattern is found also when assessing the changes in severe heat wave frequencies. Under RCP 8.5, the frequency of severe heat waves is projected to be enhanced by a factor of 6–7 compared to the modelled historical period, which corresponds to more than two events per year. The severe heat waves are projected to occur regularly (at least once per year

on average) also in the other scenarios. Nevertheless, a possible bias resulting from the overestimated severe heat wave frequencies in the historical simulations should be considered. For 2070–2099, an event with an equal or a higher magnitude than the observed 1994 heat wave is projected in a large majority (50 of 59) of model simulations. Moreover, in 30 model simulations, such an event occurs at least once per decade, indicating a considerable increase compared to the near future.

**Table 3** Projected changes in shift and scale of summer daily maximum temperature distributions and temporal autocorrelation for the near future (2020–2049) compared to their respective historical runs

	MED	P90	%	L1	L2	L3	L4	L5	L6	L7	L8	L9	L10
COR11—RCP 4.5	+1.1	+1.5	73	+0.01	+0.02	+0.02	+0.02	+0.03	+0.03	+0.03	+0.03	+0.02	+0.02
COR44—RCP 4.5	+1.3	+1.9	68	+0.05	+0.04	+0.04	+0.04	<i>+0.04</i>	<i>+0.04</i>	<i>+0.04</i>	<i>+0.04</i>	<i>+0.04</i>	<i>+0.03</i>
COR11—RCP 8.5	+1.2	+1.5	80	+0.01	+0.01	+0.01	+0.01	+0.01	+0.02	+0.02	+0.03	+0.02	+0.02
COR44—RCP 8.5	+1.3	+1.7	76	+0.04	+0.03	+0.03	+0.02	+0.03	+0.02	+0.02	+0.02	+0.03	<i>+0.03</i>
ENS22—SRES A1B	+1.3	+1.4	93	0.00	−0.01	−0.02	−0.02	−0.02	−0.02	−0.02	−0.01	−0.01	0.00

COR11 (COR44) represents EURO-CORDEX models with 0.11° (0.44°) grids and ENS22 denotes ENSEMBLES models with 0.22° grid. MED (P90) represents changes in median and the 90th percentile of summer daily maximum temperature (°C) over Central Europe. L1–L10 represents lags from 1 to 10 days, italicised values are significant at the 5% significance level. % represents percentage of the 90th percentile increase that is explained by the shift of median



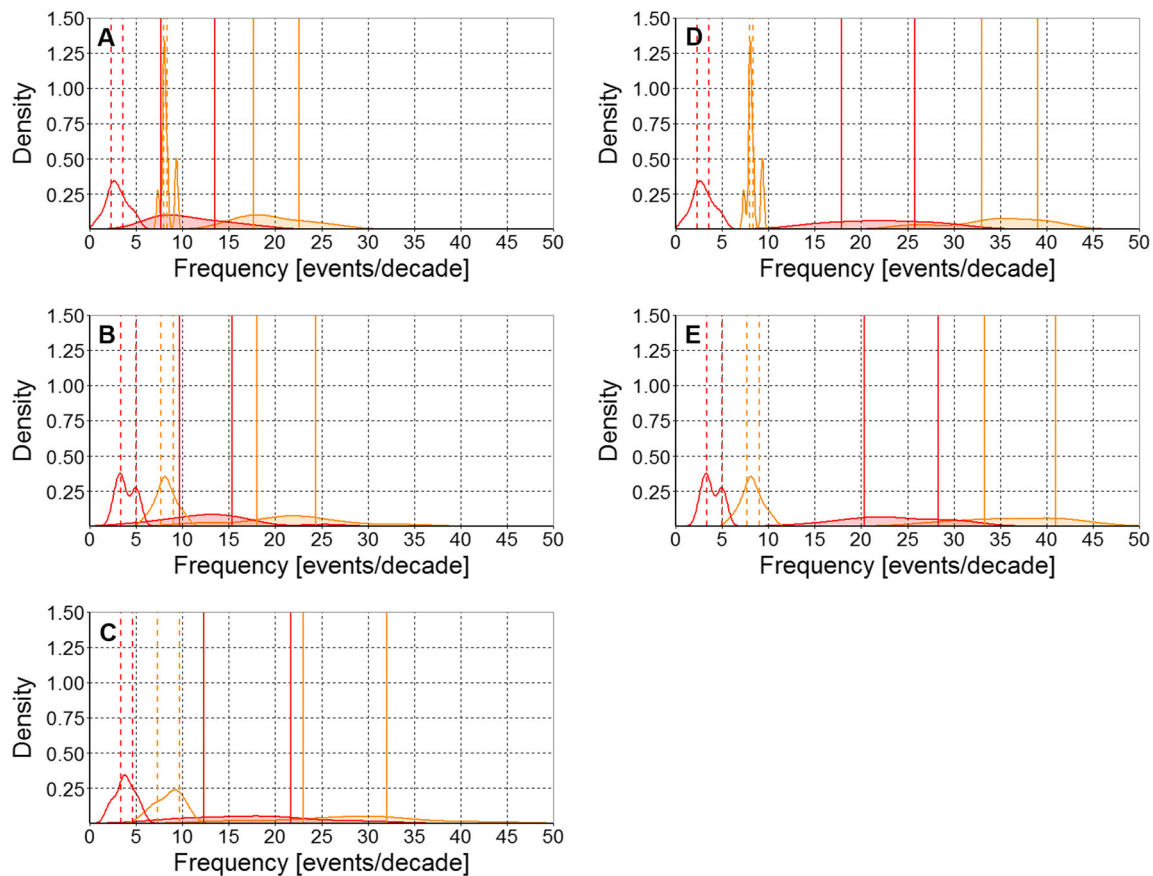


**Fig. 7** Same as Fig. 6, but for the late twenty-first century. Note the different scale of the x-axis

Alongside the substantial increase of heat wave frequencies, considerable uncertainties represented by wide IQRs and flat PDFs (Fig. 7) must be taken into account. The width of the IQRs increased roughly by a factor of 2 compared to the near future, thus indicating a large variance among the individual model simulations.

### 5 Discussion

In the observed (E-OBS) data, 5 of the 22 heat waves are regarded as ‘severe’ and may represent a type of events having particularly pronounced impacts on society and ecosystems. The 1994 heat wave is found to be the most distinctive during

the 1970–1999 period, and it was associated with large excess mortality in the Czech Republic (Kyselý and Huth 2004), Poland (Kuchcik 2001) and other Central European countries. Lhotka and Kyselý (2015a) ranked this heat wave as the most severe in Central Europe over the whole 1950–2012 period. In addition to Central Europe, this event was extraordinary also in Western Ukraine (Shevchenko et al. 2014) where it was more pronounced than the well-known 2010 heat wave. Extreme weather conditions during the summer of 1994 were also present over Western Europe (Della-Marta et al. 2007).

In the historical period, EURO-CORDEX models with the coarser 50 km grid substantially overestimated the frequency of severe heat waves, while this behaviour was improved when using their higher-resolution versions. This is in accordance

**Table 4** Same as Table 3, but for the late twenty-first century

	MED	P90	%	L1	L2	L3	L4	L5	L6	L7	L8	L9	L10
COR11—RCP 4.5	+1.9	+2.3	83	+0.01	+0.02	+0.03	+0.03	+0.04	+0.04	+0.03	+0.03	+0.03	+0.03
COR44—RCP 4.5	+2.1	+2.7	78	+0.05	+0.04	+0.03	+0.03	+0.04	+0.03	<b>+0.03</b>	+0.03	<b>+0.04</b>	<b>+0.04</b>
COR11—RCP 8.5	+3.8	+4.6	83	<b>+0.02</b>	<b>+0.03</b>	+0.03	+0.04	<b>+0.04</b>	<b>+0.04</b>	<b>+0.04</b>	+0.03	+0.03	+0.02
COR44—RCP 8.5	+4.2	+5.6	75	<b>+0.06</b>	+0.05	+0.05	<b>+0.05</b>	<i>+0.06</i>	<i>+0.05</i>	<i>+0.06</i>	<b>+0.05</b>	<i>+0.06</i>	<b>+0.05</b>
ENS22—SRES A1B	+3.5	+4.0	88	0.00	−0.01	−0.01	0.00	−0.01	−0.01	−0.01	0.00	+0.01	+0.02

The italicised values are significant at the 1% significance level; the bolded values are significant at the 5% significance level

with Vautard et al. (2013), who showed that the number of heat waves persisting more than a few days is overestimated in the EURO-CORDEX models, but this feature is improved using the 12.5 km version of the RCMs. Vautard et al. (2013) supposed this characteristic to be linked to the simulation of precipitation. This is in line with Kotlarski et al. (2014), who demonstrated that majority of EURO-CORDEX models with the 50 km grid exhibit drier summer conditions compared to their higher-resolution versions. A possible mechanism may be related to a better representation of orography in COR11, which is important for proper function of convective schemes in the relatively complex terrain of Central Europe. Smoothed elevation in the coarser (50 km) grid in COR44 provides less occasions for orographic convection (Im et al. 2010) and may contribute to more frequent precipitation deficits that amplify a heat wave's severity (e.g. Fischer et al. 2007). In addition, RCMs with the coarser grid have lower proportion of resolved precipitation compared to higher-resolution models (Rauscher et al. 2010), and thus, more precipitable water is processed through their convective scheme and they are more prone to errors originating from these sub-grid processes.

Another possible mechanism contributing to the overestimated frequency of severe heat waves relates to atmospheric circulation. Plavcová and Kysely (2016) concluded that overly persistent circulation in ENSEMBLES RCMs (driven by reanalysis) contributes to the overestimated frequency of long heat waves. The pronounced persistence of circulation patterns might be present also in our study, because the overestimated temporal autocorrelation of  $T_{\max}$  for lags of 5 days and longer was found in all model groups. Although an event comparable to the most severe 1994 heat wave was simulated only in few RCMs in the historical period, it is nevertheless necessary to consider to what extent such extreme events are typical for the recent climate and thus whether they should be simulated in RCMs driven by GCMs.

In the near future, the largest increase in variance of the  $T_{\max}$  distribution was found in EURO-CORDEX models forced by the 'low' RCP 4.5 concentration scenario. In general, the increased variance of the  $T_{\max}$  distribution might originate from changes in surface energy budget, soil moisture and atmospheric circulation (Fischer and Schär 2009). It is possible that extreme temperatures might be enhanced in models forced by the RCP 4.5 scenario due to drier summer conditions and suppressed latent cooling, thus resulting in a longer upper tail of the  $T_{\max}$  distribution compared to RCP 8.5. The lowest increment of the heat wave frequency was present in ENSEMBLES simulations, which corresponds with only a small positive change of the scale parameter. This little change in spread of the  $T_{\max}$  distribution for the ENSEMBLES RCMs was found also by Fischer and Schär (2010), who showed only a small increase of standard deviation in the mid-twenty-first century.

The late twenty-first century is characterized by a substantial increase in heat wave frequencies, which is linked to ERF

and is the largest under the RCP 8.5 scenario. Analogous results were obtained by Jacob et al. (2014) using EURO-CORDEX models forced by both RCP 4.5 and 8.5 scenarios. The scale parameter is less important in this period compared to the near future, which corresponds to Ballester et al. (2010), who concluded that future changes in Central European heat waves are expected mostly to follow summer mean warming. Using ENSEMBLES models forced by the SRES A1B concentration scenario, Fischer and Schär (2010) projected 13 heat waves per decade over Central Europe at the end of the twenty-first century. Because their definition of heat waves was based on six-day temporal criteria, this frequency is rather comparable to severe heat waves in our study and matches our results quite well.

## 6 Summary and conclusions

We analysed 62 regional climate model simulations from the ENSEMBLES and EURO-CORDEX projects in order to assess possible changes in Central European heat waves under climate change scenarios for the late twenty-first century along with related uncertainties. The main results can be summarized as follows:

In the historical period (1970–1999), all model groups simulate better the frequency of all heat waves compared to severe heat waves. The observed frequency of heat waves is close to or within IQRs of simulations in individual model groups, while the frequency of severe heat waves in RCMs is considerably overestimated. The EURO-CORDEX RCMs with the 12.5 km grid perform better with respect to the simulation of severe heat waves than their low resolution (50 km grid) versions.

In the near future (2020–2049) simulations, the frequency of heat waves is projected to be nearly twice higher compared to the historical period, while the frequency of severe heat waves increases by a factor of 2–3. The largest uncertainty originates from the selection of models. Differences between the concentration scenarios are small in this period, and the largest effective radiative forcing in RCP 8.5 is not associated with the highest frequency of heat waves.

The largest increase of heat wave frequency in the EURO-CORDEX RCMs under the RCP 4.5 scenario in the near future is related to positive changes in temporal autocorrelation and relatively large change in the scale parameter of the  $T_{\max}$  distribution, while the smallest increment in the ENSEMBLES RCMs under SRES A1B is linked to negative changes in temporal autocorrelation of  $T_{\max}$  and only a small positive change in the scale parameter of the  $T_{\max}$  distribution.

For the late twenty-first century (2070–2099), the largest uncertainty relates to the concentration scenario. Under RCP 8.5, 3–4 heat waves per summer are projected, compared to about two heat waves under RCP 4.5. Roughly two severe heat waves per summer are found on average for the RCP 8.5 simulations, and they are projected to become a regular

phenomenon (once per summer on average) also under the other scenarios.

The substantial increase of heat waves under RCP 8.5 is connected not only with the largest shift of the  $T_{\max}$  distribution but also with significant positive changes in temporal autocorrelation of  $T_{\max}$ , especially for lags of 5 days and more. Changes in the scale parameter of the  $T_{\max}$  distribution are less important than in the near future.

Extraordinary heat waves such as the one that occurred in 1994 are projected to be still rather rare in the near future, but the large majority of RCMs simulate at least one event per decade in the late twenty-first century.

The enhanced occurrence of heat waves in a future climate is robust and was found under all concentration scenarios. This emphasizes an importance to implement suitable adaptation strategies, such as those recommended by the European Climate Adaptation Platform (<http://climate-adapt.eea.europa.eu>). Designing green spaces and corridors in urban areas, supporting urban farming and gardening, performing agroforestry and crop diversification, improving water retention in agricultural areas and establishing early warning systems would mitigate impacts of heat waves in a changing climate.

**Acknowledgements** The study was supported by the Czech Science Foundation, project 16-22000S, and the Charles University Grant Agency, student project no. 250215. The EURO-CORDEX simulations were carried out in several groups within the framework of the IMPACT2C FP7 project. The ENSEMBLES simulations were obtained from the ENSEMBLES project database funded within the EU-FP6. We also acknowledge the E-OBS data set from the same project, the data providers in the ECA&D project, and the National Sustainability Program I (NPU I), grant number LO1415 from the Ministry of Education, Youth and Sports of the Czech Republic.

## References

- Amell NW, Livermore MJL, Kovats S, Levy PE, Nicholls R, Parry ML, Gaffin SR (2004) Climate and socio-economic scenarios for global-scale climate change impacts assessments: Characterising the SRES storylines. *Glob Environ Chang* 14:3–20. doi:10.1016/j.gloenvcha.2003.10.004
- Ballester J, Rodó X, Giorgi F (2010) Future changes in Central Europe heat waves expected to mostly follow summer mean warming. *Clim Dyn* 35:1191–1205. doi:10.1007/s00382-009-0641-5
- Barriopedro D, Fischer EM, Luterbacher J, Trigo RM, García-Herrera R (2011) The hot summer of 2010: redrawing the temperature record map of Europe. *Science* 332:220–224. doi:10.1126/science.1201224
- Bastos A, Gouveia CM, Trigo RM, Running SW (2014) Analysing the spatio-temporal impacts of the 2003 and 2010 extreme heatwaves on plant productivity in Europe. *Biogeosciences* 11:3421–3435. doi:10.5194/bg-11-3421-2014
- Beniston M, Stephenson DB, Christensen OB, Ferro CAT, Frei C, Goyette S, Halsnaes K, Holt T, Jylhä K, Koffi B, Palutikof J, Schöll R, Semmler T, Woth K (2007) Future extreme events in European climate: an exploration of regional climate model projections. *Clim Chang* 81:71–95. doi:10.1007/s10584-006-9226-z
- Coumou D, Rahmstorf S (2012) A decade of weather extremes. *Nat Clim Chang* 2:491–496. doi:10.1038/nclimate1452
- Davin EL, Stöckli R, Jaeger EB, Levis S, Seneviratne SI (2011) COSMO-CLM2: a new version of the COSMO-CLM model coupled to the community land model. *Clim Dyn* 37:1889–1907. doi:10.1007/s00382-011-1019-z
- Della-Marta PM, Haylock MR, Luterbacher J, Wanner H (2007) Doubled length of western European summer heat waves since 1880. *J Geophys Res* 112:D15103. doi:10.1029/2007JD008510
- Déqué M, Somot S, Sanchez-Gomez E, Goodess CM, Jacob D, Lenderink G, Christensen OB (2012) The spread amongst ENSEMBLES regional scenarios: regional climate models, driving general circulation models and interannual variability. *Clim Dyn* 38: 951–964. doi:10.1007/s00382-011-1053-x
- Deser C, Phillips A, Bourdette V, Teng H (2012) Uncertainty in climate change projections: the role of internal variability. *Clim Dyn* 38: 527–546. doi:10.1007/s00382-010-0977-x
- Deutscher Wetterdienst (DWD) (2015) August: record temperature: 40.3 °C in Kitzingen on 5 July and on 7 August 2015. [http://www.dwd.de/EN/climate\\_environment/climatechange/climatechange\\_node.html](http://www.dwd.de/EN/climate_environment/climatechange/climatechange_node.html). Accessed 27 October 2015
- Fink AH, Brücher T, Krüger A, Leckebusch GC, Pinto JG, Ulbrich U (2004) The 2003 European summer heatwaves and drought—synoptic diagnosis and impacts. *Weather* 59:209–216. doi:10.1256/wea.73.04
- Fischer EM, Seneviratne SI, Lüthi D, Schär C (2007) Contribution of land-atmosphere coupling to recent European summer heat waves. *Geophys Res Lett* 34:L06707. doi:10.1029/2006GL029068
- Fischer EM, Schär C (2009) Future changes in daily summer temperature variability: driving processes and role for temperature extremes. *Clim Dyn* 33:917–935. doi:10.1007/s00382-008-0473-8
- Fischer EM, Schär C (2010) Consistent geographical patterns of changes in high-impact European heatwaves. *Nat Geosci* 3:398–403. doi:10.1038/ngeo866
- Fischer EM, Knutti R (2015) Anthropogenic contribution to global occurrence of heavy-precipitation and high-temperature extremes. *Nat Clim Chang* 5:560–565. doi:10.1038/NCLIMATE2617
- Hawkins E, Sutton R (2009) The potential to narrow uncertainty in regional climate predictions. *Bull Am Meteorol Soc* 90:1095–1107. doi:10.1175/2009BAMS2607.1
- Haylock MR, Hofstra N, Klein Tank AMG, Klok EJ, Jones PD, New M (2008) A European daily high-resolution gridded data set of surface temperature and precipitation for 1950–2006. *J Geophys Res* 113: D20119. doi:10.1029/2008JD010201
- Heinrich G, Gobiet A, Mendlik T (2014) Extended regional climate model projections for Europe until the mid-twentyfirst century: combining ENSEMBLES and CMIP3. *Clim Dyn* 42:521–535. doi:10.1007/s00382-013-1840-7
- Holtanová E, Valeriánová A, Crhová L, Racko S (2015) Heat wave of august 2012 in the Czech Republic: comparison of two approaches to assess high temperature event. *Stud Geophys Geod* 59:159–172. doi:10.1007/s11200-014-0805-6
- Hoy A, Hänsel S, Skalák P, Ustrnul Z, Bochniček O (2016) The extreme European summer of 2015 in a long-term perspective. *Int J Climatol*. doi:10.1002/joc.4751
- Hurrell JW, Deser C (2010) North Atlantic climate variability: the role of the North Atlantic oscillation. *J Mar Syst* 79:231–244. doi:10.1016/j.jmarsys.2009.11.002
- Iglesias A, Quiroga S, Moneo M, Garrote L (2012) From climate change impacts to the development of adaptation strategies: challenges for agriculture in Europe. *Clim Chang* 112:143–168. doi:10.1007/s10584-011-0344-x
- Im ES, Coppola E, Giorgi F, Bi X (2010) Validation of a high-resolution regional climate model for the alpine region and effects of a subgrid-scale topography and land use representation. *J Clim* 23:1854–1873. doi:10.1175/2009JCLI3262.1
- Jacob D, Petersen J, Eggert B, Alias A, Christensen OB, Bouwer LM, Braun A, Colette A, Déqué M, Georgievski G, Georgopoulou E, Gobiet A, Menut L, Nikulin G, Haensler A, Hempelmann N,

- Jones C, Keuler K, Kovats S, Kröner N, Kotlarski S, Kriegsmann A, Martin E, van Meijgaard E, Moseley C, Pfeifer S, Preuschmann S, Radermacher C, Radtke K, Rechid D, Rounsevell M, Samuelsson P, Somot S, Soussana J-F, Teichmann C, Valentini R, Vautard R, Weber B, Yiou P (2014) EURO-CORDEX: new high-resolution climate change projections for European impact research. *Reg Environ Chang* 14:563–578. doi:10.1007/s10113-013-0499-2
- Kjellström E, Bärring L, Jacob D, Jones R, Lenderink G, Schär C (2007) Modelling daily temperature extremes: recent climate and future changes over Europe. *Clim Chang* 81:249–265. doi:10.1007/s10584-006-9220-5
- Kjellström E, Boberg F, Castro M, Christensen JH, Nikulin G, Sánchez E (2010) Daily and monthly temperature and precipitation statistics as performance indicators for regional climate models. *Clim Res* 44:135–150. doi:10.3354/cr00932
- Kjellström E, Nikulin G, Hansson U, Strandberg G, Ullerstig A (2011) Twenty-first century changes in the European climate: uncertainties derived from an ensemble of regional climate model simulations. *Tellus A* 63:24–40. doi:10.1111/j.1600-0870.2010.00475.x
- Kononov IB, Beekmann M, Kuznetsova IN, Yurova A, Zvyagintsev AM (2011) Atmospheric impacts of the 2010 Russian wildfires: integrating modelling and measurements of an extreme air pollution episode in the Moscow region. *Atmos Chem Phys* 11:10031–10056. doi:10.5194/acp-11-10031-2011
- Kotlarski S, Keuler K, Christensen OB, Colette A, Déqué M, Gobiet A, Goergen K, Jacob D, Lüthi D, van Meijgaard E, Nikulin G, Schär C, Teichmann C, Vautard R, Warrach-Sagi K, Wulfmeyer V (2014) Regional climate modeling on European scales: a joint standard evaluation of the EURO-CORDEX RCM ensemble. *Geosci Model Dev* 7:1297–1333. doi:10.5194/gmd-7-1297-2014
- Kuchcik M (2001) Mortality in Warsaw: is there any connection with weather and air pollution? *Geogr Pol* 74:29–45
- Kyselý J, Huth R (2004) Heat-related mortality in the Czech Republic examined through synoptic and “traditional” approaches. *Clim Res* 25:265–274
- Kyselý J (2010) Recent severe heat waves in central Europe: how to view them in a long-term prospect? *Int J Climatol* 109:89–109. doi:10.1002/joc1874
- Lau NC, Nath MJ (2014) Model simulation and projection of European heat waves in present-day and future climates. *J Clim* 27:3713–3730. doi:10.1175/JCLI-D-13-00284.1
- Lemonsu A, Beaulant A, Somot S, Masson V (2014) Evolution of heat wave occurrence over the Paris basin (France) in the twenty-first century. *Clim Res* 61:75–91. doi:10.3354/cr01235
- Lhotka O, Kyselý J (2015a) Characterizing joint effects of spatial extent, temperature magnitude and duration of heat waves and cold spells over Central Europe. *Int J Climatol* 35:1232–1244. doi:10.1002/joc.4050
- Lhotka O, Kyselý J (2015b) Hot central-European summer of 2013 in a long-term context. *Int J Climatol* 35:4399–4407. doi:10.1002/joc.4277
- Lhotka O, Kyselý J (2015c) Spatial and temporal characteristics of heat waves over Central Europe in an ensemble of regional climate model simulations. *Clim Dyn* 45:2351–2366. doi:10.1007/s00382-015-2475-7
- Meehl GA, Tebaldi C (2004) More intense, more frequent, and longer lasting heat waves in the twenty-first century. *Science* 305:994–997. doi:10.1126/science.1098704
- Moss RH, Edmonds JA, Hibbard KA, Manning MR, Rose SK, van Vuuren DP, Carter TR, Emori S, Kainuma M, Kram T, Meehl GA, Mitchell JFB, Nakicenovic N, Riahi K, Smith SJ, Stouffer RJ, Thomson AM, Weyant JP, Wilbanks TJ (2010) The next generation of scenarios for climate change research and assessment. *Nature* 463:747–756. doi:10.1038/nature08823
- Nikulin G, Kjellström E, Hansson U, Strandberg G, Ullerstig A (2011) Evaluation and future projections of temperature, precipitation and wind extremes over Europe in an ensemble of regional climate simulations. *Tellus A* 63A:41–55. doi:10.1111/j.1600-0870.2010.00466.x
- Plavcová E, Kyselý J (2011) Evaluation of daily temperatures in Central Europe and their links to large-scale circulation in an ensemble of regional climate models. *Tellus A* 63A:763–781. doi:10.1111/j.1600-0870.2011.00514.x
- Plavcová E, Kyselý J (2016) Overly persistent circulation in climate models contributes to overestimated frequency and duration of heat waves and cold spells. *Clim Dyn* 46:2805–2820. doi:10.1007/s00382-015-2733-8
- Prather M, Flato G, Friedlingstein P, Jones C, Lamarque J-F, Liao H, Rasch P (2013) Annex II: climate system scenario tables. *Clim. Chang. 2013 Phys. Sci. Basis. Contrib. Work. Gr. I to Fifth Assess. Rep. Intergov. Panel Clim. Chang*
- Rauscher SA, Coppola E, Piani C, Giorgi F (2010) Resolution effects on regional climate model simulations of seasonal precipitation over Europe. *Clim Dyn* 35:685–711. doi:10.1007/s00382-009-0607-7
- Riahi K, Rao S, Krey V, Cho C, Chirkov V, Fischer G, Kindermann G, Nakicenovic N, Rafaj P (2011) RCP 8.5—a scenario of comparatively high greenhouse gas emissions. *Clim Chang* 109:33–57. doi:10.1007/s10584-011-0149-y
- Robine J-M, Cheung SLK, Le Roy S, Van Oyen H, Griffiths C, Michel J-P, Herrmann FR (2008) Death toll exceeded 70,000 in Europe during the summer of 2003. *C R Biol* 331:171–178. doi:10.1016/j.crv.2007.12.001
- Schneiderreit A, Schubert S, Vargin P, Lunkeit F, Zhu X, Peters DHW, Fraedrich K (2012) Large-scale flow and the long-lasting blocking high over Russia: summer 2010. *Mon Weather Rev* 140:2967–2981. doi:10.1175/MWR-D-11-00249.1
- Shevchenko O, Lee H, Snizhko S, Mayer H (2014) Long-term analysis of heat waves in Ukraine. *Int J Climatol* 34:1642–1650. doi:10.1002/joc.3792
- Silver NC, Dunlap WP (1987) Averaging correlation coefficients: should Fisher’s z transformation be used? *J Appl Psychol* 72:146–148
- Strandberg G, Bärring L, Hansson U, Jansson C, Jones C, Kjellström E, Kolax M, Kupiainen M, Nikulin G, Samuelsson P, Ullerstig A, Wang S (2014) CORDEX scenarios for Europe from the Rossby Centre regional climate model RCA4. *Rep Meteorol Climatol. ISSN: 0347-2116*
- Thomson AM, Calvin KV, Smith SJ, Kyle GP, Volke A, Patel P, Delgado-Arias S, Bond-Lamberty B, Wise MA, Clarke LE, Edmonds JA (2011) RCP4.5: a pathway for stabilization of radiative forcing by 2100. *Clim Chang* 109:77–94. doi:10.1007/s10584-011-0151-4
- van der Linden P, Mitchell JFB (2009) ENSEMBLES: climate change and its impacts: summary of research and results from the ENSEMBLES project. *Met Office Hadley Centre, Exeter*
- van Vuuren DP, Edmonds J, Kainuma M, Riahi K, Thomson A, Hibbard K, Hurtt GC, Kram T, Krey V, Lamarque J-F, Masui T, Meinshausen M, Nakicenovic N, Smith SJ, Rose SK (2011) The representative concentration pathways: an overview. *Clim Chang* 109:5–31. doi:10.1007/s10584-011-0148-z
- Valerianová A, Crhová L, Holtanová E, Kašpar M, Müller M, Pecho J (2015) High temperature extremes in the Czech Republic 1961–2010 and their synoptic variants. *Theor Appl Climatol*. doi:10.1007/s00704-015-1614-8
- Vautard R, Gobiet A, Jacob D, Belda M, Colette A, Déqué M, Fernández J, García-Díez M, Goergen K, Güttler I, Halenka T, Karacostas T, Katragkou E, Keuler K, Kotlarski S, Mayer S, van Meijgaard E, Nikulin G, Patarčić M, Scinocca J, Sobolowski S, Suklitsch M, Teichmann C, Warrach-Sagi K, Wulfmeyer V, Yiou P (2013) The simulation of European heat waves from an ensemble of regional climate models within the EURO-CORDEX project. *Clim Dyn* 41:2555–2575. doi:10.1007/s00382-013-1714-z
- Zentralanstalt für Meteorologie und Geodynamik (ZAMG) (2013) New temperature record: 40.5 °C in Bad Deutsch-Altenburg. <http://www.zamg.ac.at/cms/de/klima/news/neuer-hitze-rekord-40-5deg-c-in-baddeutsch-altenburg>. Accessed 16 January 2014.